The AAPS Journal, Vol. 13, No. 4, December 2011 (© 2011)
DOI: 10.1208/s12248-011-9298-1

Research Article

Relationships between Liposome Properties, Cell Membrane Binding, Intracellular Processing, and Intracellular Bioavailability

Yinghuan Li,[1,2] Jie Wang,[3] Yue Gao,[2] Jiabi Zhu,[1] M. Guillaume Wientjes,[2] and Jessie L.-S. Au[2,4]

Received 12 May 2011; accepted 23 August 2011; published online 10 September 2011

Abstract. Positive surface charge enhances liposome uptake into cells. Pegylation, used to confer stealth properties to enable *in vivo* applications of cationic liposomes, compromises internalization. The goal of this study was to determine the quantitative relationships between these two liposome properties (separately and jointly), liposomes binding to cell membrane, and the subsequent internalization and residence in intracellular space (referred to as intracellular bioavailability). The results, obtained in pancreatic Hs-766T cancer cells, revealed nonlinear and inter-dependent relationships, as well as substantial qualitative and quantitative differences. The proportionality constant K of intracellular and membrane-bound liposomes at equilibrium (i.e., I_{eq} and B_{eq}) showed a positive triphasic relationship with surface charge and a negative biphasic relationship with pegylation. Near-neutral liposomes showed little internalization of the membrane-bound moiety, increasing to a constant *K* value for medium charge liposomes (+15 to +35 mV zeta potential), followed by a further increase for highly charged liposomes (greater than or equal to +46 mV). The decline of pegylation with *K* value showed a breakpoint at 2%. The negative consequences of pegylation (%PEG) were partially offset by increasing charge (ZP). The best-fitting regression equations are: $B_{eq}=-1.36\times\%PEG+0.33\times ZP$; $I_{eq}=-1.52\times\%PEG+0.34\times ZP$. It suggested that 1% pegylation increase can be offset with 4 mV ZP. The differences are such that it may be possible to balance these parameters to simultaneously maximize the stealth property and intracellular bioavailability of cationic liposomes.

KEY WORDS: cationic liposomes; internalization; membrane binding; pegylation; zeta potential.

[1] Division of Pharmaceutics, College of Pharmacy, China Pharmaceutical University, Nanjing 210009, Jiangsu, People's Republic of China.
[2] Division of Pharmaceutics, College of Pharmacy, The Ohio State University, 500 West 12th Ave, Columbus, Ohio 43210, USA.
[3] Optimum Therapeutics LLC, OSU Science Tech Village, Columbus, Ohio 43212, USA.
[4] To whom correspondence should be addressed. (e-mail: au.1@osu.edu)

ABBREVIATIONS: AUC, Area-under-concentration-time curve; *B* and B_{eq}, Concentration of liposomes bound to cell membrane at time *t* and at equilibrium; C*X*-*Y*, Cationic liposomes with *X* mol.% DOTAP and *Y*% pegylation; DAPI, 4′,6-Diamidino-2-phenylindole, dihydrochloride; DOPE, 1,2-Dioleoyl-sn-glycero-3-phosphoethanolamine; DOTAP, 1,2-Dioleoyl-3-trimethylammonium-propane; DPPC, 1,2-Dipalmitoyl-sn-glycero-3-phosphocholine; EC, Initial extracellular concentration; EPR, Enhanced permeability and retention; *I* and I_{eq}, Intracellular concentrations of liposomes at time *t* and at equilibrium; mPEG-DSPE, 1,2-Distearoyl-sn-glycero-3-phosphoethanolamine-*N*-[methoxy(polyethylene glycol)-2000]; PBS, Phosphate-buffered saline; PEG, Polyethylene glycol; PEG-DSPE, 1,2-Distearoyl-sn-glycero-3-phosphoethanolamine-*N*-carbamoyl-methoxypoly-ethylene glycol-2000; Rhod-DOPE, DOPE-*N*-(lissamine rhodamine B sulfonyl) ammonium salt; TC and TC_{eq}, Total concentrations of cell-associated liposomes at time *t* and at equilibrium; T_{eq}, Time to reach equilibrium; ZP, Zeta potential.

INTRODUCTION

The intended target sites for gene therapeutics are located intracellularly, e.g., in the cytoplasm for siRNA (1) or in the nucleus for DNA (2). The physicochemical properties of nucleic acids (i.e., large molecular size, hydrophilic, negative charge) block their entry into cells. Effective *in vitro* transfection is achieved by formulating gene therapeutics in cationic gene vectors that, due to their positive charges, facilitate the internalization of nucleic acids. Among this group, cationic liposomes are intensively investigated due to their biocompatibility and the relative simplicity of their production in laboratory and large-scale quantities (reviewed in (1,3–5)). Cationic liposomes form complexes (lipoplexes) with nucleic acids through electrostatic interaction. The net charge of the lipoplexes is determined by the charge ratio between cationic liposomes and nucleic acids, which is in turn determined by the cationic lipid content (mol.%) and the number of negatively charged phosphate groups on the DNA/RNA backbone. This net charge affects the particle size, structure, stability, and transfection efficiency of lipoplexes (6). Further enhancement of internalization of cationic liposomes is achieved with modifications using other components, such as cell penetrating peptides (1) and membrane

permeable ligands (7), usually through conjugation with one of the lipids.

On the *in vivo*, whole body level, particles such as cationic liposomes are rapidly cleared by the reticuloendothelial system (1). This problem is partially resolved by coating the liposomal surface using polyethylene glycol (PEG) to confer stealth property. A longer circulation time in turn promotes the passive tumor targeting *via* the enhanced permeability and retention (EPR) effect caused by the leaky vasculature and absence of lymphatic drainage in tumors (8). The extent of pegylation is usually controlled by the concentration of PEG in liposomes. For example, the FDA-approved pegylated liposomal doxorubicin (Doxil®) comprises 5% pegylated lipids (PEG-DSPE or 1,2-distearoyl-sn-glycero-3-phosphoethanolamine-*N*-carbamoyl-methoxypolyethylene glycol-2000), in addition to two neutral lipids (hydrogenated soy phosphatidylcholine at 56% and cholesterol at 38%) (9). In general, the extent of pegylation can be varied from 0.5% to 15% without affecting the structural stability of the phospholipid bilayer (10–12). On the other hand, pegylation compromises the internalization of liposomes due to (a) inhibition of opsonization (binding between liposomes and proteins), (b) increased surface hydrophilicity, and (c) neutralization of the positive surface charge required for binding to the negatively charged cell surface.

In view of the opposing effects of positive surface charge and pegylation on the ability of liposomal gene carriers to reach intracellular target sites, a better understanding of the quantitative relationships between these parameters and the kinetic processes that determine the fate of these carriers in intracellular compartments may enable their optimization. The goal of the current study was to determine the effects of these two liposome properties, separately and jointly, on the kinetics of liposome binding to cell membrane and internalization and residence in intracellular space (referred to as intracellular bioavailability). 1,2-Dioleoyl-3-trimethylammoniumpropane (DOTAP) was chosen as a model cationic lipid, because it has been used for delivering siRNA (13) and DNA (14), and has been tested in humans (15). Liposomes with positive surface charges ranging from +4 to +56 mV were obtained using different DOTAP mol.% (without nucleic acids). Pegylation was achieved using the methoxy analog of PEG-DSPE. Human pancreatic Hs-766T cancer cells were used as the model cell system. The results revealed nonlinear and inter-dependent effects of positive surface charge and pegylation on cell membrane binding and intracellular processing of cationic liposomes. The quantitative data further indicates the possibility to fine-tune these properties to simultaneously maximize the stealth property and intracellular bioavailability of cationic liposomes.

MATERIALS AND METHODS

Materials

DOTAP, 1,2-dioleoyl-sn-glycero-3-phosphoethanolamine (DOPE), 1,2-dipalmitoyl-sn-glycero-3-phosphocholine (DPPC), 1,2-dioleoyl-sn-glycero-3-phospho-ethanolamine-*N*-(lissamine rhodamine B sulfonyl) ammonium salt (Rhod-DOPE), 1,2-distearoyl-sn-glycero-3-phosphoethanolamine-*N*-[methoxy(polyethylene glycol)-2000] (mPEG-DSPE), and cholesterol were purchased from Avanti Polar Lipids, Inc. (Alabaster, AL); Triton X-100 from RICCA Chemical Co. (Arlington, TX); 4′,6-diamidino-2-phenylindole, dihydrochloride (DAPI) from InVitrogen Corp. (Eugene, OR). All other reagents and solvents were of analytical or HPLC grade and were purchased from Fisher Chemicals (Pittsburgh, PA). All materials were used as received.

Cell Culture

Human pancreatic Hs-766T carcinoma cells were a gift of Dr. Byoungwoo Ryu from Johns Hopkins University (Baltimore, MD). Cells were cultured in DMEM media (Lonza, Walkersville, MD), supplemented with 90 μg/mL gentamicin, 90 μg/mL cefotaxime sodium, 1% non-essential amino acids, and 10% fetal bovine serum (FBS), and maintained in a humidified atmosphere containing 5% CO_2 at 37°C.

Liposome Preparation

We prepared several liposome formulations. The starting liposomes comprised three neutral lipids, DPPC, DOPE, and cholesterol. DPPC has negligible effect on cellular uptake of liposomes (see Results). DPPC and cholesterol were used to increase liposome stability. DOPE was used to increase the elasticity of the liposome bilayer and to promote the liposome fusion with the cell and endosomal membrane; the latter promotes the liposome release from endosomes (16). Rhod-DOPE (red fluorescence) was added to enable detection. mPEG-DSPE (0–7 mol.%) was used to achieve surface pegylation. DOTAP (5–50 mol.%) was used to provide positive surface charge.

Liposomes were prepared using the standard thin-film hydration method, followed by polycarbonate membrane extrusion (17). Briefly, Rhod-DOPE and other lipids were dissolved in chloroform and transferred into a suitable round bottom flask. The lipid film was formed under rotary evaporation and further dried overnight under vacuum. The thin film was rehydrated with 10% sucrose in water to yield a final lipid concentration of 10 mg/ml. The lipid suspension was then passed through a polycarbonate membrane (100 nm pore size) 11 times with an extruder (Avanti, Alabaster, AL); this resulted in a particle size of between 100 and 150 nm, a size commonly used to benefit from the EPR effect in tumors (18,19).

Liposome size distribution and zeta-potential (ZP) were determined on a Zetasizer Nano ZS90 (Malvern, Westborough, MA, USA). Liposomes were diluted with serum-free DMEM to yield stock solutions containing 5, 10, 20, 50, 100, and 200 μg/ml of total lipid.

Confocal Fluorescence Microscopic Analysis of Cell Membrane Binding and Intracellular Bioavailability of Liposomes

We evaluated the temperature dependence of liposome binding and internalization. Cells were seeded on coverslips placed inside a six-well plate overnight to allow the formation of a monolayer. The plates were placed on an orbital shaker and cells were incubated with rhodamine-labeled liposomes

at a final medium concentration of 50 μg/ml lipids at 37°C and 4°C for 6 h, washed three times with ice-cold phosphate-buffered saline (PBS), and fixed in 10% formalin solution for 20 min. After staining the cell nuclei with DAPI (0.6 μg/ml in PBS, 20 min staining), the coverslip was transferred to a glass slide and examined under a confocal microscope (Olympus FluoView™ FV1000, Hamburg, Germany). The excitation/emission wavelengths were 401/421 and 543/594 nm for DAPI (blue) and rhodamine (red), respectively.

Cell Membrane Binding and Intracellular Bioavailability: Experimental Methods

Cells were seeded in six-well plates, allowed to reach a density of about 1×10^6 cells/well, washed once with PBS and incubated with 1 ml DMEM at 37°C for 30 min. After replacing the medium with a suspension of rhodamine-labeled liposomes, the plates were incubated on an orbital shaker at 37°C or 4°C for 0–6 h. Changes in the extracellular liposome concentrations over time were measured for liposomes comprising 20 and 40 mol.% DOTAP. At predetermined time points, culture medium (containing free liposomes not associated with cells) was removed, and the attached cells were washed three times with ice-cold PBS. Both culture medium and cells were then solubilized (to yield soluble rhodamine) by incubating with 0.5 ml of 0.5% Triton-X 100 in PBS for 30 min at 37°C and further diluted to 1 ml with PBS. The fluorescence intensities of the resulting solutions were measured on a LS 55 Fluorescence Spectrometer (Perkin Elmer, Waltham, MA). The fluorescence intensity was converted to amount of cell-associated liposomes using standard curves constructed with known amounts of rhodamine-labeled liposomes.

Several studies have demonstrated that the amount of cell-associated PLGA nanoparticles and liposomes at 4°C represents the amount bound to cell membrane (i.e., no internalization) (20–22). To determine if the same observation applies to the current liposomes, we compared the amount of cell-associated liposomes at 4°C to the amount of membrane-bound liposomes at 37°C. The latter was determined using a published method (23). Briefly, cells were incubated with liposomes (C40-0) at 4°C and 37°C. Afterward, cells treated at 37°C were washed three times with ice-cold PBS and incubated with a 10× trypsin solution for 30 min at 37°C to dissociate the membrane-bound liposomes (confirmed with confocal microscopy, manuscript in preparation). The mixture was centrifuged at 1,000×*g* (4°C, 20 min); the supernatant contained the free liposomes (dissociated from cells) and the pellet contained cells (with internalized liposomes). After solubilization with Triton-X 100, the fluorescence in the two fractions was determined. The results confirmed that the amount of membrane-bound liposomes at 37°C was indistinguishable from the amount of cell-associated liposomes at 4°C (see "RESULTS").

Cell Membrane Binding and Intracellular Bioavailability: Data Analysis

The time course of changes in cell-associated liposomes was used to determine the time to reach equilibrium binding (T_{eq}); this time point was used in subsequent studies. Binding and internalization was differentiated based on temperature-dependent changes. As internalization is an active process, only binding occurred at 4°C, while both binding and internalization took place at 37°C (20). The total concentration of cell-associated liposomes in cells treated at 37°C represented the sum of cell membrane-bound and intracellular liposomes (TC). The concentration at 4°C represented the membrane-bound liposomes (B), and the difference between TC and B represented the intracellular concentration (I). This temperature-dependent binding/uptake was confirmed by confocal microscopy studies (see "RESULTS").

To determine the effects of surface charge and pegylation on the internalization of membrane-bound liposomes and subsequent intracellular processing, we plotted I *versus* B at T_{eq} (I_{eq} and B_{eq}) obtained at several initial extracellular concentrations (from 5 to 200 μg/ml), for individual liposome formulations. The slope of the resulting regressed line for each formulation equals K, the proportionality constant between I_{eq} and B_{eq}.

$$\frac{I_{eq}}{B_{eq}} = K$$

We used K as an overall measure of intracellular accumulation of liposomes, inclusive of internalization, intracellular degradation, and efflux. We used K for several reasons: (a) K values were calculated from I_{eq} and B_{eq}; such values are less variable compared to the initial slopes (hence better data quality), (b) K was determined using the slope of several observations over a wide range of initial extracellular liposome concentrations and, hence, represents averaged values that are less prone to data variability, and (c) analysis of the composite intracellular bioavailability and binding data for a large number of samples with very different liposome properties, i.e., different surface charges and different pegylation, enables the analysis of the qualitative and quantitative effects of these parameters on the nature and mechanisms of internalization and intracellular processing of membrane-bound liposomes (see "RESULTS").

The area-under-concentration-time curve (AUC) was calculated using the trapezoidal rule. Statistical significance of the difference among multiple groups was analyzed using the Tukey test after ANOVA. Linear regression was performed with the SAS routine Proc Reg (SAS, Cary, NC).

RESULTS

Properties of Cationic Liposomes

For this report, the tested liposomes are referred to as C*X*-*Y*, with *X* and *Y* being the mol.% of DOTAP and mPEG-DSPE, respectively. For example, C20-1 refers to 20 mol.% DOTAP and 1% pegylation. These and other properties of the cationic liposomes used in the present study are shown in Table I. All liposomes showed a narrow size distribution with mean particle sizes of 125–145 nm and polydispersity indices of less than 0.2. Increasing pegylation from 0% to 7% yielded <10% increase in particle size. ZP values positively correlated with the content of DOTAP (Fig. 1a). Pegylation slightly reduced the ZP values, e.g., from 46.2 mV at 0%

Table I. Properties of Cationic Liposomes

Composition C*X*-*Y*[a]	DOTAP (%)	mPEG-DSPE (%)	DPPC (%)	Cholesterol (%)	Size (nm)	Poly-dispersity index	Zeta potential (mV)
C0-0	0	0	30	50	126	0.04	4.1
C5-0	5	0	25	50	128	0.06	17.5
C10-0	10	0	20	50	133	0.07	21.8
C20-0	20	0	10	50	132	0.07	35.7
C40-0	40	0	0	40	135	0.09	46.2
C50-0	50	0	0	30	131	0.11	56.2
C20-1	20	1	9	50	133	0.07	35.4
C20-2	20	2	8	50	136	0.09	32.8
C20-5	20	5	5	50	140	0.09	30.9
C40-1	40	1	0	39	136	0.10	45.4
C40-2	40	2	0	38	137	0.08	44.4
C40-3.5	40	3.5	0	36.5	140	0.14	42.1
C40-5	40	5	0	35	142	0.06	40.8
C40-7	40	7	0	33	142	0.16	39.3

All formulations contained 1% rhodamine-labeled DOPE and 19% DOPE
[a] *X* = mol.% DOTAP, *Y* = mol.% PEG

pegylation to 39.3 mV at 7%, for C40-*Y* liposomes (Fig. 1b). The latter is likely due to the negatively charged phosphate group of mPEG-DSPE as previously reported (24).

In several studies, liposomes containing the 50 mol.% DOTAP were also tested. However, we observed significant cytotoxicity with more than 60% of cells detached from the growth surface upon incubation beyond 2 h. This, in turn, prohibited accurate quantitative measurements of liposomal binding and uptake. In contrast, cells treated with lower DOTAP concentrations (5–40 mol.%) remained viable over the duration of experimentation. Data obtained with liposomes with lower DOTAP concentrations were used in the analyses.

Cell Membrane Binding and Internalization of Cationic Liposomes: Confocal Microscopy Results

Figure 2 shows the confocal microscopy images of liposome-treated pancreatic Hs-766T cells at 6 h, at 4°C and 37°C. Comparison of these images shows that at 37°C, the red fluorescence signals were observed on the cell membrane and inside the cell. In comparison, at 4°C, the fluorescence signals were present only on the cell membrane. These results confirmed that concentrations of cell-associated liposomes at 4°C and 37°C represented the concentration of membrane-bound liposomes (*B*) and the total concentration (TC, sum of membrane-bound and intracellular liposomes), respectively. The difference between these two values represents the concentration of intracellular (*I*) liposomes. Note that the intracellular liposomes were present primarily in the cytosol, with little or no fluorescence in the nuclei. In general, the levels of membrane-bound and intracellular liposomes increased with surface charge and decreased with pegylation, consistent with literature reports.

Of particular interest are the changes in the intracellular locations and appearance of the fluorescence signals caused by increasing surface charge and pegylation (see results obtained at 37°C). First, with respect to surface charge (see data for C*X*-0), the starting liposome C0-0 showed minimal association with cells. Addition of 5 or 10 mol.% of DOTAP increased the membrane-bound liposomes more extensively compared to the intracellularly located liposome (C5-0 and C10-0 groups), whereas further increases to 20 or 40 mol.% enhanced both the membrane-bound and intracellular liposomes (C20-0 and C40-0 groups). The latter two groups also showed more even intracellular distribution with fluorescence signals dispersed throughout the cytosol. In contrast, the lower charge C5-0 and C10-0 groups showed primarily clusters of liposomes near the cell membrane.

Second, pegylation altered the appearance of the fluorescence signals, i.e., fluorescence signals at higher pegylation were increasingly punctated (e.g., compare C20-5 to C20-0 and C40-7 to C40-1). The most obvious shifts occurred at 2%

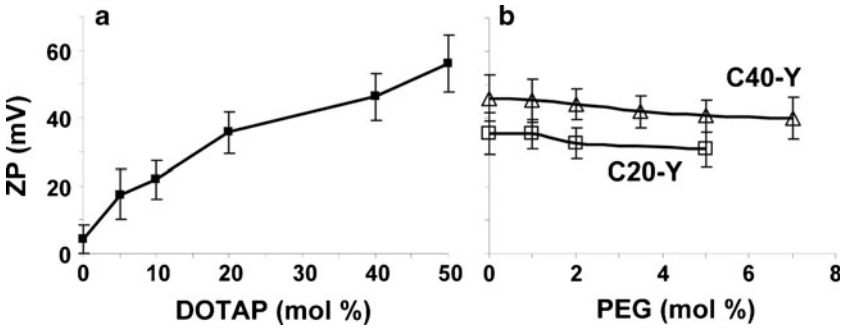

Fig. 1. Effects of cationic lipid content and % pegylation on liposome surface charge (ZP). C*X*-*Y* *X* = mol.% DOTAP, *Y* = mol.% PEG. Mean ± SD, *n*=3

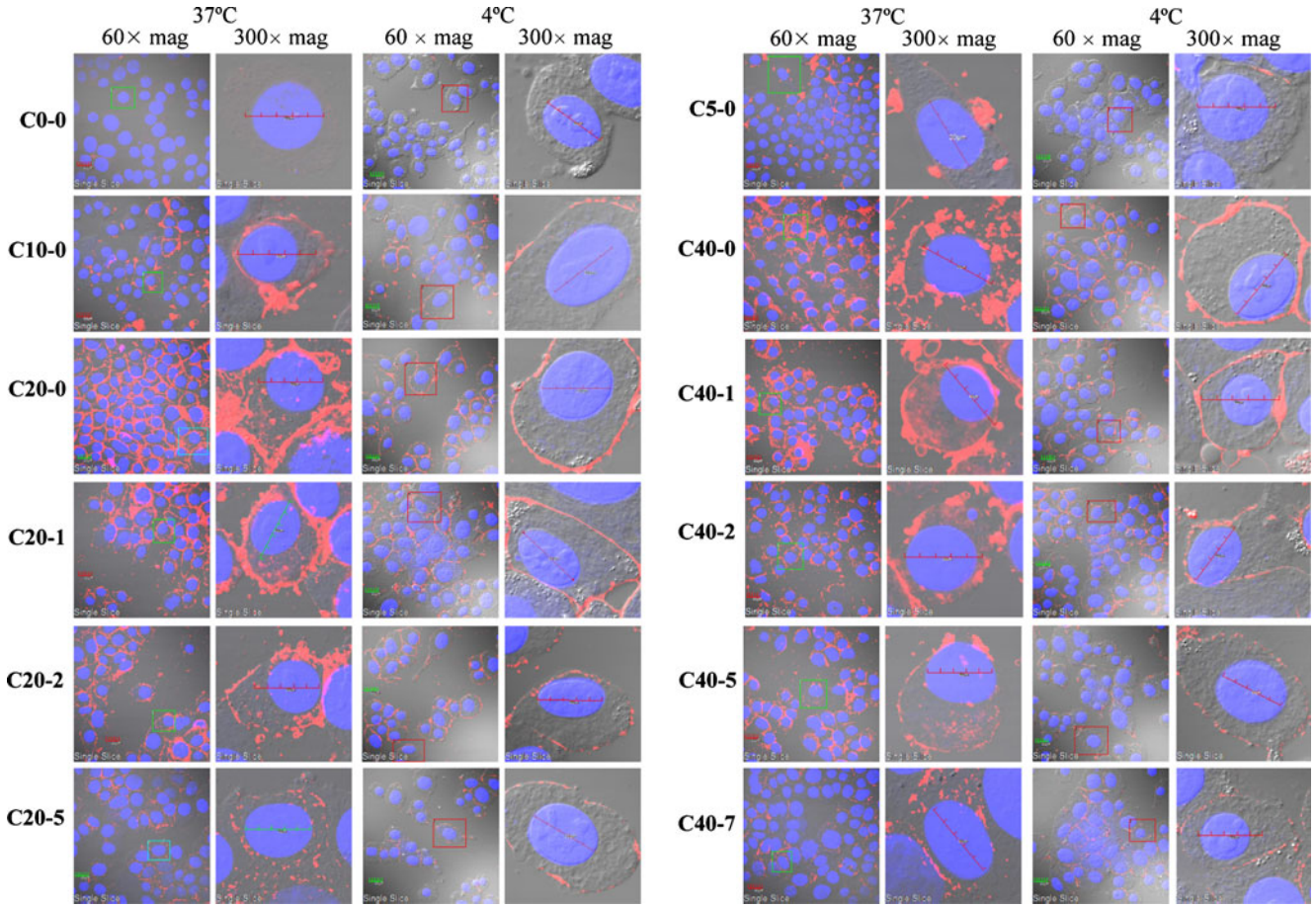

Fig. 2. Cellular uptake of cationic liposomes: confocal microscopy results. Cells were incubated with liposomes for 6 h at 37°C and 4°C, in Hs 766T cells. C*X*-*Y* *X* = mol.% DOTAP, *Y* = mol.% PEG. Mean ± SD, $n=3$. Rhodamine-labeled liposomes appear in *red fluorescence*, nuclei appear in *blue fluorescence*. *Bar* 20 μm. Single cell images correspond to cells in *rectangles* from group images. Overlay by DIC light with *red* and *blue* filters

pegylation. Endocytosed particles such as liposomes travel from the membrane to perinuclear locations *via* the endosomal transport and can be released into the cytosol during this transport. Punctated signals generally indicate liposome localization in endosomes, whereas liposomes released into the cytosol would yield more diffused signals. Hence, the increasingly punctated signals suggest that pegylation alters the intracellular processing of the endocytosed liposomes.

The results in Fig. 2 also show the combined effects of pegylation. For the liposomes with higher positive surface charges (C20-*Y* and C40-*Y*), while increasing pegylation to 5% or 7% progressively decreased the cell-associated liposomes, their presence in the cell remained apparent. This is qualitatively different from the C5-0 and C10-0 liposomes, which resided mainly on or close to the cell membrane. This difference in liposome localization (intracellularly dispersed *vs*. membrane localized) occurred even though these different types of liposomes yielded relatively similar TC, *B*, and *I* levels (e.g., compare C5-0 and C10-0 to C20-5, C40-5 and C40-7, see below).

Kinetics of Uptake, Cell Membrane Binding, and Internalization of Cationic Liposomes: General Findings

Table II compares the amount of cell-associated liposomes at 4°C to the amount of cell membrane-bound liposomes at 37°C; the results indicate comparable values. This finding is consistent with several reports (20–22) and confirms that the internalized amount (*I*) can be calculated as the difference between the total cell-associated amount obtained at 37°C (TC) and the cell-associated amount obtained at 4°C (*B*).

Figure 3 shows the time-dependent accumulation of cell-associated liposomes comprising different surface charges and different % pegylation. The concentrations of liposomes are shown as TC, *B*, and *I*. Note that *I* represents all intracellular liposomes, which is the net of several kinetic processes (i.e., internalization of membrane-bound liposomes and subse-

Table II. The Amount of Cell-Associated Liposomes at 37°C and 4°C

C40-0	Cell-associated liposomes[a] for 1 h (%)
37°C, total	100
37°C, binding	41.5±0.7
37°C, internalization	59.3±1.1
4°C, total	41.0±1.1

[a] Cell-associated liposomes were described as the relative fluorescence intensities (divided by the total fluorescence intensity at 37°C) per cell. Data shown are mean values ± SD ($n=3$)

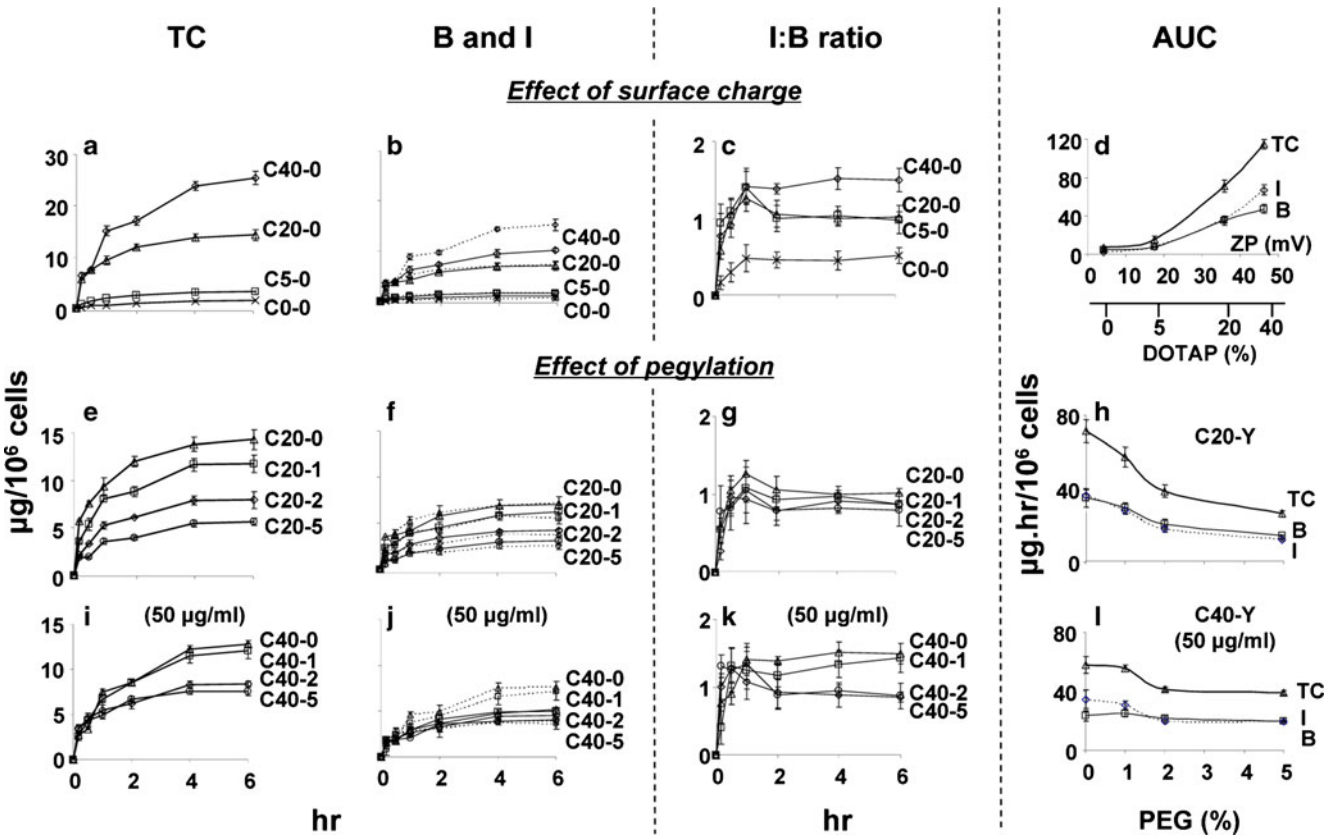

Fig. 3. Effect of surface charge and pegylation on membrane-binding and intracellular bioavailability: time course study. *TC* concentration of cell-associated total liposomes, *B* concentration of membrane-bound liposomes, *I* concentration of internalized liposomes, *I*/*B* ratios and AUC were calculated. C*X*-*Y* *X* = mol.% DOTAP, *Y* = mol.% PEG. Mean ± SD, n=3. Some SD are smaller than *symbols*. **a**–**c** Liposomes without pegylation. C0-0 (*ex symbol*), C5-0 (*square*), C20-0 (*triangle*), and C40-0 (*diamond*). **e**–**g** C20-*Y* liposomes with 0-5% pegylation. C20-0 (*triangle*), C20-1 (*square*), C20-2 (*diamond*), C20-5 (*circle*). **i**–**k** C40 liposomes with 0–5% pegylation. C40-0 (*triangle*), C40-1 (*square*), C40-2 (*diamond*), C40-5 (*circle*). **d** Effect of surface charge on AUC of TC, **b**, **i** the *x*-axis represents ZP and the corresponding mol.% DOTAP. **h**, **l** Effect of pegylation on AUC of TC, **b**, **i** for C20-*Y* and C40-*Y* liposomes. For all figures: *solid lines* denote the *B* values and *dotted lines* denote the *I* values. The initial extracellular liposome concentration was 100 μg/ml, except where indicated

quent processing such as endosomal transport, lysosomal degradation, and efflux or recycling). The results are summarized in Table III. In all cases, the amounts of fluorescence increased with time and reached plateau levels at about 4 h, indicating 4 h as the time to reach equilibrium, T_{eq}. Initial extracellular liposome concentrations were 100 μg/ml for most studies. For evaluation of the effect of pegylation, initial concentrations of 50 μg/ml were used for C40-*Y* liposomes. This was to achieve similar amounts of cell-associated liposomes for C40-*Y* and C20-*Y* liposomes and to eliminate potential concentration-dependent differences.

For most liposomes, the time-dependent changes in *I* values were similar to corresponding changes in *B* values, as shown by the similar shapes of the curves (Fig. 3b, f, j). Interestingly, *I* values were about equal to *B* values for nearly all liposomes. The two exceptions were C40-0 and C40-1 liposomes, where *I* values exceeded *B* values at all time points. This kinetic data, expressed as function of time, provided the first indication of different kinetics of internalization and intracellular processing for the C40-0 and C40-1 liposomes compared to other liposomes with lower surface charge (C0-*Y* to C20-*Y*) or at the same surface charge but higher pegylation (C40-2 and C40-5).

Figure 4 shows the changes of extracellular concentrations of C20-0 and C40-0 liposomes upon incubation with cells at 37°C. As expected, the concentration declined over time, due to uptake into cells. In all cases, the decline leveled off at about 2 to 4 h. The kinetics of liposome accumulation in cells is inversely related to the kinetics of extracellular concentration decline. We calculated the mass balance using the amounts of plateau TC levels (Fig. 3) and the remaining extracellular liposomes (Fig. 4), at 4 h, and accounted for 90±10% and 92±9% of the initial amounts (for C20-0 and C40-0 liposomes). The ~10% loss was likely due to transfer, washing procedures, and adsorption to contact surfaces.

Effects of Positive Surface Charge

Figure 3a and b shows the effects of surface charge on the kinetics of the three entities of cell-associated liposomes (TC, *B*, and *I*). Table III summarizes the levels of these entities at T_{eq} and their corresponding cumulative values over time (i.e., AUC from 0 to 6 h). These results show increasing

Table III. Effects of Surface Charge and Pegylation on Liposome Binding and Intracellular Bioavailability

	Plateau value at 4~6 h (μg/10^6 cells)			AUC (μg h/10^6 cells)			*I*/*B* ratio	
Composition C*X*-*Y*[a]	TC_{eq}	B_{eq}	I_{eq}	TC	*B*	*I*	I_{eq}/B_{eq}	AUC of *I*/AUC of *B*
Effect of surface charge (initial extracellular concentration was 100 μg/ml)								
C0-0	1.61	1.06	0.55	6.80[b]	4.65[b]	2.20[b]	0.46	0.47
C5-0	3.23	1.63	1.60	15.5[b]	7.55[b,d]	7.92[b]	1.01	1.05
C20-0	14.3	7.07	7.22	71.5[b]	35.1[b]	36.4[b]	1.03	1.04
C40-0	25.4	10.2	15.3	115[b]	47.5[b]	67.2[b]	1.50	1.41
Effect of pegylation on C20-*Y* (initial extracellular concentration was 100 μg/ml)								
C20-0	14.3	7.07	7.22	71.5	35.1	36.4	1.03	1.04
C20-1	11.7	6.26	5.50	57.4[c]	29.5[c]	27.9[c]	0.93	0.95
C20-2	7.93	4.22	3.72	38.8[c]	20.7[c]	18.1[c]	0.90	0.87
C20-5	5.65	3.13	2.52	26.4[c]	14.4[c]	12.0[c]	0.81	0.83
Effect of pegylation on C40-*Y* (initial extracellular concentration was 50 μg/ml)								
C40-0	12.8	5.14	7.65	57.9	23.4	34.5	1.49	1.47
C40-1	12.1	4.96	7.12	55.5	24.5	31.0	1.39	1.27
C40-2	8.41	4.54	3.87	41.3[c]	21.5	19.9[c]	0.89	0.93
C40-5	7.59	4.05	3.54	39.1[c]	19.8[c]	19.3[c]	0.88	0.97

TC concentration of total cell-associated liposomes; *B* concentration of cell membrane-bound liposomes; *I* concentration of intracellular liposomes

The corresponding concentrations at equilibrium are TC_{eq}, B_{eq}, and I_{eq}, and were obtained after 4 h incubation. Area-under-concentration-time profiles from time 0 to 6 h were calculated using the trapezoidal rule

[a] *X* = mol.% DOTAP, *Y* = mol.% PEG

[b] Differences among multiple groups of C*X*-0 were significant ($p<0.01$, ANOVA/Tukey)

[c] Differences between C20-0 and C20-*Y*, and between C40-0 and C40-*Y* were statistically significant ($p<0.01$, ANOVA/Tukey)

[d] Exception is the AUC of B between C0-0 and C5-0 ($p>0.05$, ANOVA/Tukey)

TC, *B*, and *I* levels with increasing positive surface charge and with time.

Figure 3c shows the changes of *I*/*B* ratios with time; the results identified two noteworthy observations. First, the *I*/*B* ratios initially increased with time, up to 1 h, followed by a decrease at 2 h. For the liposomes with lower positive charge (C5-0 and C20-0), the ratios remained at the lower plateau levels from 2 to 6 h. The liposomes with higher positive charge (C40-0) behaved differently; the ratios resumed their increase over time, reaching a higher plateau level at 4–6 h. Second, the *I*/*B* ratios increased with DOTAP mol.% and ZP values in a nonlinear manner. The *I*/*B* ratio was less than 0.5 for the neutral C0-0 liposomes, increasing to about 1 for C5-0 and C20-0 liposomes, and to about 1.5 for C40-0 liposomes (Table III). These data suggest that high positive surface charge increases the effectiveness of internalization, resulting in increased intracellular bioavailability.

Figure 3d compares the AUC value of TC, *B*, and *I*. The results, summarized in Table III, confirm the greater increase in *I* relative to *B* at higher positive surface charge (i.e., AUC of *I* exceeded AUC of *B* for C40-0).

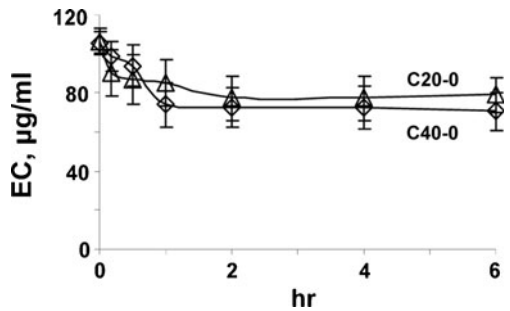

Fig. 4. Changes of extracellular liposomal concentration (*EC*) over time. Initial EC is 100 μg/ml

Effects of Pegylation

The above results indicate significant differences for liposomes comprising 20 and 40 mol.% DOTAP. Hence, we used these two liposomes to study the effects of pegylation. In all cases, the levels of TC, *B*, and *I* increased with time and decreased with increasing pegylation (Fig. 3e, f, i, j).

All C20-*Y* liposomes, irrespective of the extent of pegylation, showed similar kinetics in the changes in *I*/*B* ratios, i.e., an initial increase during the first hour, followed by a decrease at 2 h to reach lower plateau levels of between 0.8 and 1.1 from 2 to 6 h (Fig. 3g). On the other hand, the C40-*Y* liposomes showed more complex kinetics that was dependent on % pegylation; the liposomes with higher pegylation (C40-2 and C40-5) displayed the same kinetics and similar *I*/*B* ratios as the C20-*Y* liposomes. In contrast, the liposomes with no or 1% pegylation (C40-0 and C40-1) showed very different kinetics; the ratios for both liposomes resumed increases after 2 h and both showed the same higher plateau levels of about 1.5 (Fig. 3k). These data are in agreement with the confocal microscopy data.

Figure 3h and l compares the AUC values of TC, *B*, and *I* for C20-*Y* (ZP of +35 mV) and C40-*Y* (ZP of +46 mV) liposomes, obtained at a single extracellular concentration (100 and 50 μg/ml, respectively) and at different % pegylation. The results show the inter-dependent effects of positive surface charge and pegylation. Decreases in AUC of all three entities due to pegylation were more extensive at medium charge than at high charge (i.e., decrease corresponding to increase in pegylation from 0% to 5% was, on average, ~2.7-fold for C20-*Y* *vs.* ~1.5-fold for C40-*Y*). Also noteworthy is

the separation of the AUC of *I* from the AUC of *B* for the C40-0 and C40-1 liposomes, whereas all other formulations showed overlapping values.

Comparisons of Effects of Positive Surface Charge and Pegylation

Table III compares the quantitative differences in TC, *B*, and *I* levels at 4~6 h and accumulation over 6 h, as functions of changes in surface charge and pegylation. Within the experimental conditions, the magnitude of changes due to positive surface charge is generally much greater compared with changes in pegylation. For example, TC, *B*, and *I* showed ~16-, 10-, and 28-fold difference between C0-0 and C40-0 liposomes, compared with ~2.5-, 2.3-, and 2.9-fold difference between 0% and 5% pegylation for C20-*Y* liposomes. As indicated above, the magnitudes of changes for C40-*Y* liposomes due to pegylation (from 0% to 5%, ~1.7-, 1.3-, and 2.2-fold decrease for TC, *B*, and *I*) are generally lower than for C20-*Y* liposomes. These data indicate greater effects of surface charge on the three kinetic processes, relative to pegylation.

Figure 5 shows the concentration-dependent accumulation of cell-associated liposomes, at 4 h. While TC_{eq}, B_{eq}, and I_{eq} (representing TC, *B*, and *I* at 4 h) generally increased with extracellular liposome concentrations, the increases appeared saturable at higher concentrations and greater increases were observed for the more highly charged liposomes.

Surface charge and pegylation also showed different effects on cell membrane binding and internalization. The relationships between B_{eq} and initial extracellular concentration (EC) for all non-pegylated liposomes are close to linear (Fig. 5a), indicating primarily non-saturable binding. In contrast, upon increasing pegylation, the B_{eq} *versus* EC relationships showed an increasing degree of saturation, suggesting pegylation caused a switch to saturable membrane binding.

To determine whether and to what extent the effects of the decreases due to pegylation can be offset by increasing the surface charge, we compared the TC_{eq}, B_{eq}, and I_{eq} levels obtained at 200 μg/ml extracellular concentrations (Table IV). The results indicate comparable TC, *B*, and *I* levels for the following pairs, i.e., C20-1 *vs*. C10-0, C40-3.5 or C40-5 *vs*. C10-0, and C40-7 *vs*. C20-5. This quantitative comparison indicates that the negative consequences of increasing pegylation can be partly offset by increasing the surface charge. To obtain a quantitative estimate of the increase in surface charge required to offset a change in pegylation, we determined the best-fitting linear regression equation (without intercept) relating I_{eq} to pegylation (%PEG) and ZP. This equation is: $I_{eq} = -1.52 \times \%PEG + 0.34 \times ZP$, with $R^2 = 0.96$. This indicates that, in first approximation, 1% pegylation increase can be offset with (1.52/0.34=) 4.5 mV ZP. A similar

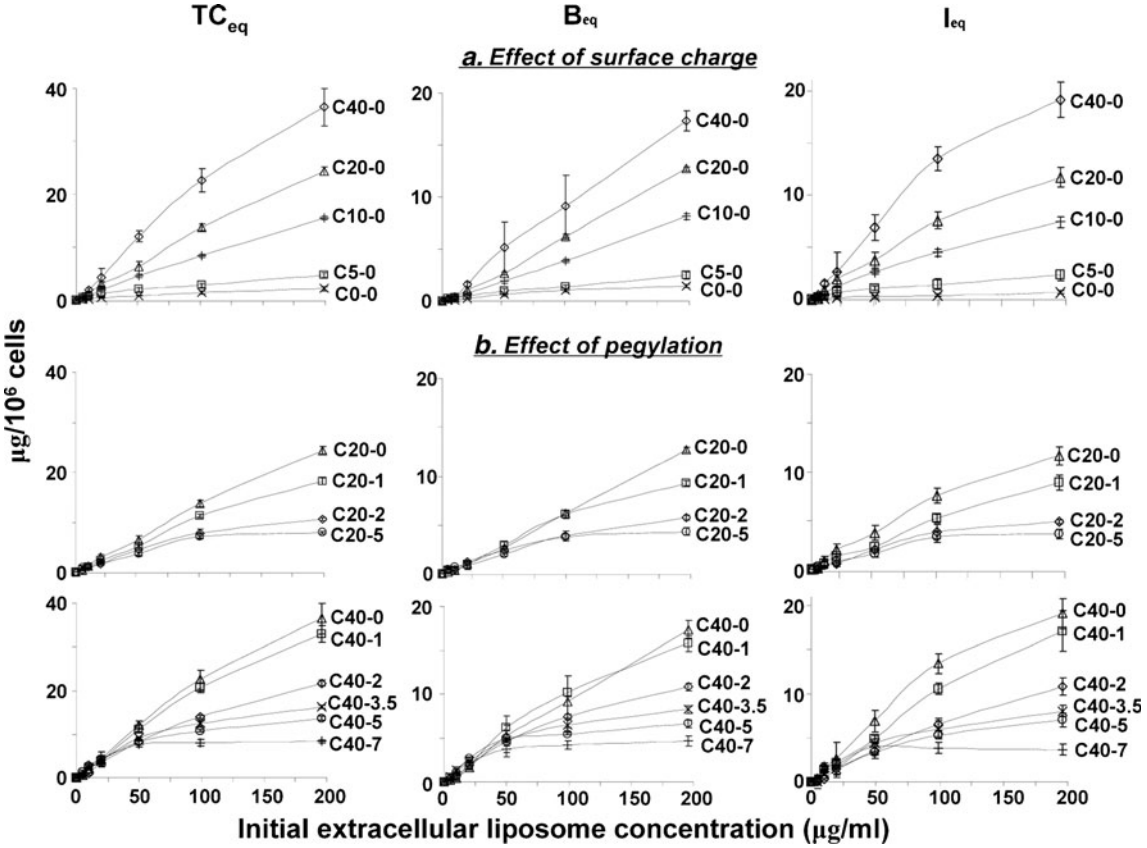

Fig. 5. **a**, **b** Concentration-dependent membrane binding and intracellular bioavailability at equilibrium: Effects of surface charge and pegylation. Data were obtained after incubation for 4 h or T_{eq}. TC_{eq} concentration of cell-associated total liposomes at T_{eq}, B_{eq} concentration of membrane-bound liposomes at T_{eq}, I_{eq} concentration of internalized liposomes at T_{eq}. C*X*-*Y* *X* = mol.% DOTAP, *Y* = mol.% PEG. Mean ± SD, *n*=3. Some SD are smaller than *symbols*. Note the different scales for *y*-axis for the three entities

Table IV. Intracellular Liposomes *versus* Membrane-Bound Liposomes: Effects of Surface Charge and Pegylation

Composition C*X*-*Y*[a]	Plateau value at 4 h (μg/10^6 cells), at 200 μg/ml initial extracellular concentrations		
	TC_{eq}	B_{eq}	I_{eq}
Effect of surface charge			
C0-0	2.15	1.46	0.69
C5-0	4.78	2.47	2.31
C10-0	15.5	8.11	7.39
C20-0	24.4	12.7	11.7
C40-0	36.5	17.4	19.1
Effect of pegylation			
C20-0	24.4	12.7	11.7
C20-1	18.1	9.26	8.86
C20-2	10.6	5.73	4.87
C20-5	7.92	4.31	3.60
C40-0	36.5	17.4	19.1
C40-1	32.9	15.8	17.1
C40-2	21.7	10.8	10.8
C40-3.5	16.3	8.26	8.04
C40-5	13.7	6.64	7.04
C40-7	8.34	4.68	3.66

[a] *X* = mol.% DOTAP, *Y* = mol.% PEG

regression shows that 1% pegylation can be offset with 4.4% DOTAP. Plots of observed *versus* predicted values of TC_{eq}, B_{eq}, and I_{eq} are shown in Fig. 6 and have coefficients of determination of 0.87~0.89. Additional 3-dimensional plots show the relationships between %PEG, ZP, and observed and predicted values of TC_{eq}, B_{eq}, and I_{eq}.

Effects of Surface Charge and Pegylation on Internalization of Membrane-Bound Liposomes and Intracellular Bioavailability

The above results showed opposing effects of positive surface charge and pegylation on liposome binding to cell membrane and intracellular bioavailability. To analyze the relationships between liposome properties and liposome internalization and subsequent intracellular processing, we plotted the values of I_{eq} *vs*. B_{eq} values obtained at 4 h and at different initial extracellular concentrations, for individual liposome formulations (i.e., data in Fig. 5). As the membrane-bound liposomes are internalized, *I* values were linearly related to *B* values; plots of I_{eq} *vs*. B_{eq} yielded the proportionality constant *K* (equals slope of the line) for each formulation. Plots of *K* values *versus* surface charge and pegylation, in turn, enabled us to determine the relationship between membrane binding and intracellular bioavailability of liposomes, as functions of surface charge and pegylation. For example, an increase in *K* with surface charge indicates the charge affects the liposome internalization plus subsequent intracellular processing to a greater extent compared to membrane binding. Conversely, a constant *K* indicates proportional changes in I_{eq} and B_{eq} and, therefore, similar effects on both components. In general, *K* increased with surface charge and decreased with pegylation (Fig. 7).

Figure 7a shows the effect of surface charge on the relationship between I_{eq} and B_{eq}. Linear regression analysis of the data points revealed three different groups with visually separate lines (each with R^2 between 0.96 and 0.98); the neutral liposomes (C0-0) showed a much lower slope of 0.46, the second group of three liposomes with medium positive surface charge (C5-0, C10-0, and C20-0) showed similar slopes of 0.99 (see the overlapping lines for the three liposomes), and the third group with high positive charge (C40-0) showed the highest slope of 1.2. These data indicate surface charge altered the kinetics of internalization and intracellular processing of membrane-bound liposomes. The *K* values calculated using these data show a triphasic plot, with >200% increase from C0-0 to C5-0 liposomes (corresponding ZP of +4 to +17 mV), no change between C5-0, C10-0, and C20-0 (ZP of +17, +22, and +35 mV), followed by ~20% increase for C40-0 (ZP of +46 mV). It is noted that additional results for C50-0 liposomes showed increases similar to those for C40-0 (not shown and not included for analysis due to the substantial cell death which compromised the data quality). These data indicate that for liposomes with ZP between +17 and +35 mV, the increase in intracellular bioavailability is proportional to the increase in membrane binding. For liposomes with ZP outside this range, the increase in intracellular bioavailability is due to additional charge-induced changes, such as enhanced internalization, lower efflux, and/or less degradation.

Figure 7b shows the effect of pegylation. Linear regression analysis of I_{eq} *versus* B_{eq} plots showed six visually separate lines (R^2 between 0.91 and 0.99). The C20-*Y* group showed three lines (one for C20-0, one for C20-1, and one for C20-2 and C20-5 jointly). The C40-*Y* group also showed three lines, one each for C40-0 and C40-1 jointly and one for C40-2, C40-3.5, C40-5, and C40-7 jointly. The slopes for the six lines ranged from 0.85 to 1.19. These data indicate pegylation affected the intracellular bioavailability of membrane-bound liposomes. The *K* values calculated using these data showed a biphasic decline, with the greatest decrease between 0% and 2% pegylation and relatively little changes for >2% pegylation. These data indicate 2% pegylation as the breakpoint above which the reduction in intracellular bioavailability is due to reduction in membrane binding. At <2% pegylation, the decrease in

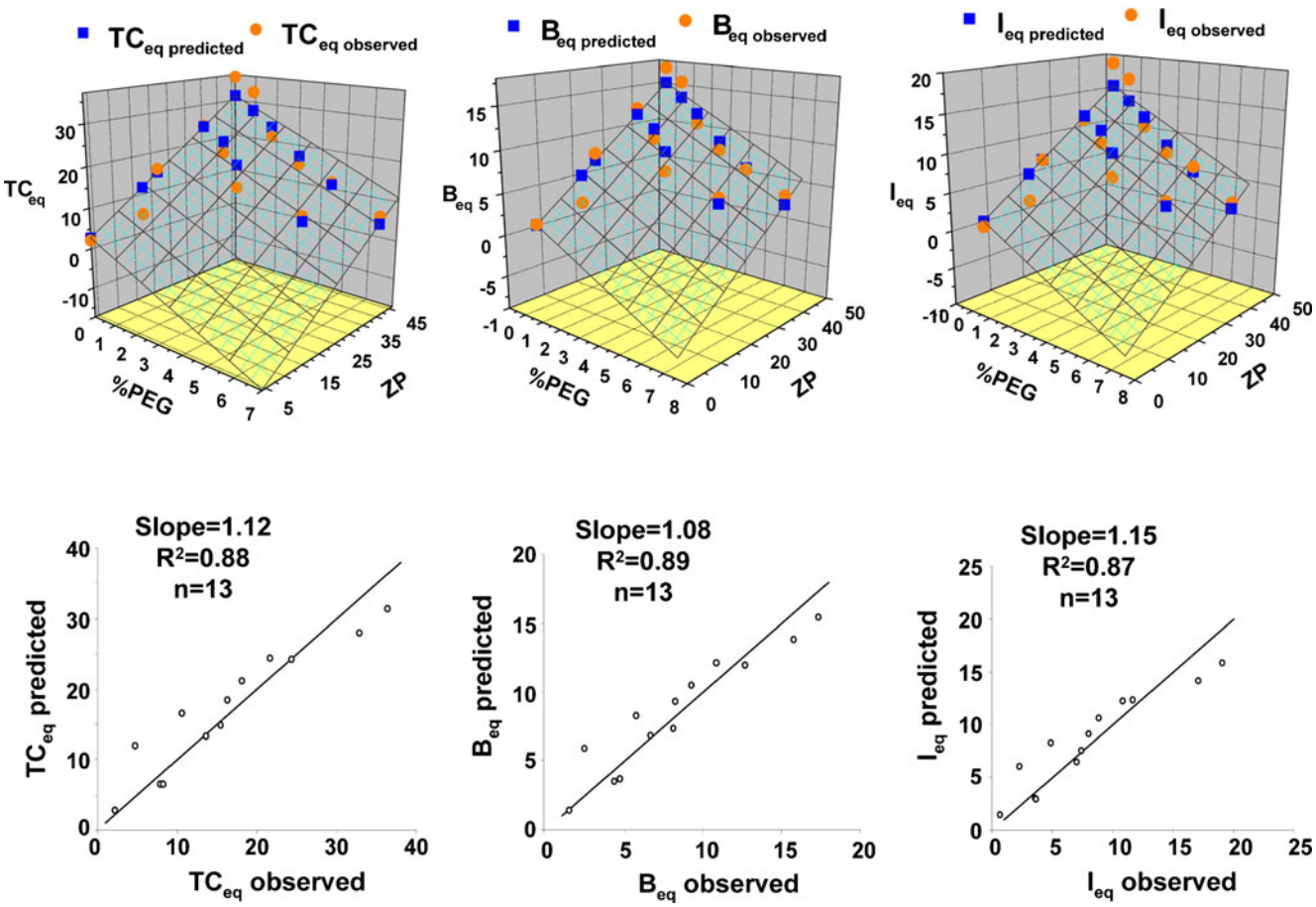

Fig. 6. Liposome binding and internationalization: surface charge and pegylation as correlates. TC_{eq} concentration of cell-associated total liposomes at equilibrium (4 h), B_{eq} concentration of membrane-bound liposomes at equilibrium (4 h), I_{eq} concentration of internalized liposomes at equilibrium (4 h). Observed values for TC_{eq}, B_{eq}, and I_{eq} from Table III were regressed with ZP and %PEG to determine the best linear regression equation without intercept. Liposome amounts as functions of ZP and %PEG are shown in *3D plots*. The relationship between regression-predicted concentrations and observed concentrations are shown in *2D plots*. Units for all concentrations are μg/10^6 cells. The regression equations, showing regression coefficients ±95% confidence limits, are: TC_{eq}, predicted=(−2.88±0.99)×%PEG+(0.68±0.08)×ZP, R^2=0.97; B_{eq}, predicted=(−1.36±0.44)×%PEG+(0.33±0.04)×ZP, R^2=0.97; I_{eq}, predicted=(−1.52±0.56)×%PEG+(0.34±0.05)×ZP, R^2=0.96

intracellular bioavailability exceeded the decrease in membrane binding, indicating lower internalization of the membrane-bound liposomes, greater efflux, or greater degradation of intracellular liposomes.

Comparison of the regressed lines for the I_{eq} *versus* B_{eq} plots indicates a more narrow range of slopes for liposomes with varying % pegylation, relative to liposomes with varying surface charge. These data indicate that changing the positive surface charge has greater impact on the internalization and intracellular processing of membrane-bound liposomes. In general, the effect of pegylation was diminished at higher surface charge, e.g., the C40-*Y* liposomes showed higher *K* values compared to the C20-*Y* liposomes with the same % pegylation, and the enhancements in *K* due to increasing the positive surface charges are more extensive compared to the reductions due to increasing pegylation (2.6-fold increase from C0-0 to C40-0 and 1.3-fold decrease from C40-0 to C40-7).

DISCUSSION

Cationic liposomes are under continued investigation as carrier of gene therapeutics. These vehicles provide excellent transfection in cultured cells but perform poorly *in vivo* after systemic delivery due to unfavorable pharmacokinetic properties. To improve the pharmacokinetic properties, the carriers are frequently pegylated. The surface properties of liposomes, i.e., surface charge and pegylation, affect the interaction with the environment in many ways. For example, increasing cationic charge results in stabilization of liposomes and also facilitates binding to negatively charged cell membranes (6). A low percentage of pegylation of less than 5% is believed to result in a loose surrounding hydrophilic structure that causes interaction and therefore aggregation of liposomes, whereas higher pegylation result in a brush-like structure with increased stability (25). Pegylation also changes the mechanism of endocytosis, e.g., clathrin-mediated endocytosis plays the primary role for uptake of unpegylated liposomes, but only a minor role for transport of pegylated liposomes (25,26). Therefore, both surface charge and pegylation can alter liposome interaction with bio-membranes, release of gene therapeutics from endosomes, and ultimately transfection. Interplay between these properties, affecting overall liposome behavior and intracellular bioavailability and efficacy of gene therapeutics is likely. Several studies have evaluated the effects of surface

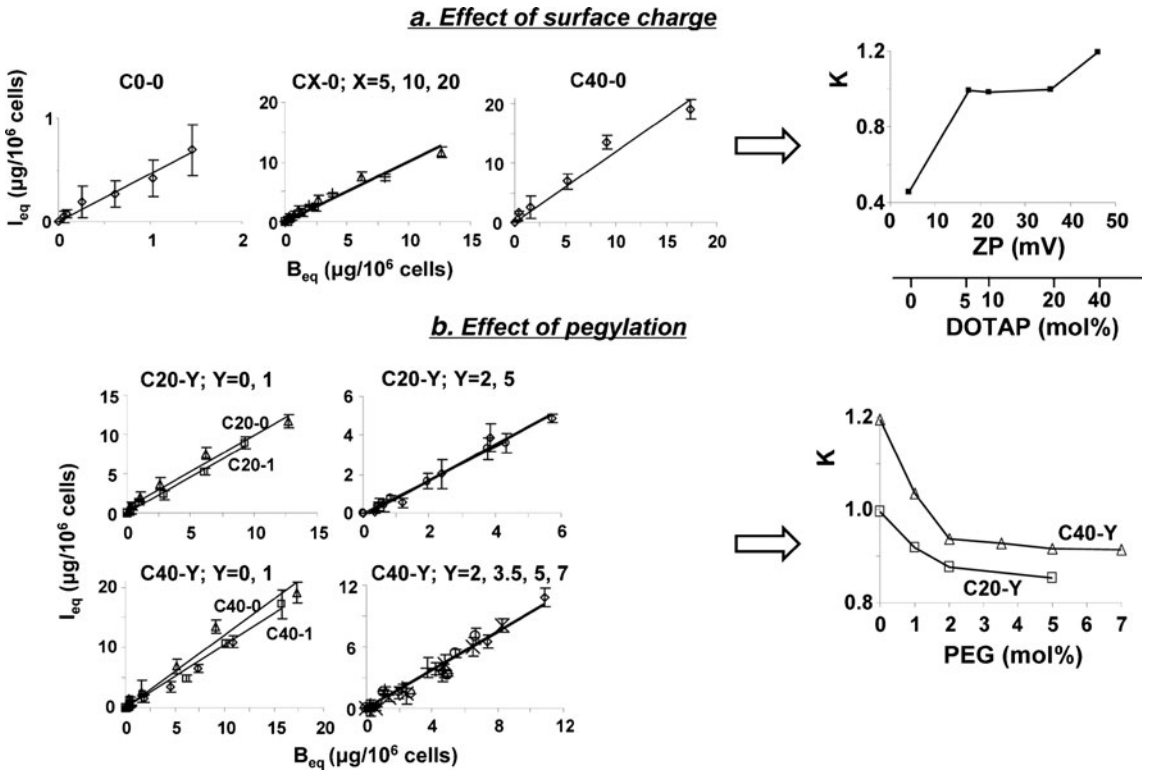

Fig. 7. Analysis of internalization of membrane-bound liposomes: effects of surface charge and pegylation on the I_{eq}-to-B_{eq} proportional constant K. Figures located on the *left of arrows* are plots of I_{eq} *versus* B_{eq} data at different initial extracellular concentrations (5 to 200 µg/ml, data shown in Fig. 5). **a** C0-0 (*diamond*), C5-0 (*square*), C10-0 (*plus sign*), C20-0 (*triangle*), C40-0 (*diamond*); **b** *triangle* C20-0/C40-0, *square* C20-1/C40-1, *diamond* C20-2/C40-2, *ex symbol* C40-3.5, *circle* C20-5/C40-5, *plus sign* C40-7. The *lines* are the best-fitted regressed lines and the *slopes* are the proportional constants K. Mean ± SD, n=3. Some SD are smaller than *symbols*. Plots of K *versus* surface charge and % pegylation are shown to the *right of arrows*. Additional results for C50-0 liposomes showed increases similar to those for C40-0 (not shown, see text)

charge and pegylation on transfection, sometimes including kinetic measurements (27,28), but few have evaluated the combined effects of surface properties on cell membrane binding and internalization of liposomes and the subsequent intracellular processing. Such studies are needed to gain insight in approaches to balance *in vivo* pharmacokinetic behavior with maximizing the intracellular bioavailability of candidate gene therapeutics.

The goal of the present project was to determine the relationships between surface charge and pegylation of cationic liposomes and the kinetics of the various processes that determine the intracellular bioavailability (i.e., binding to cell membrane and subsequent internalization, intracellular transport, and intracellular processing). We systematically altered the surface charge (ZP from +4 to +46 mV) and pegylation (from 0% to 7%) of rhodamine-labeled liposomes, separately and jointly, and used them to quantify the levels of membrane binding and intracellular bioavailability. We further used confocal microscopy to examine the intracellular distribution/dispersion.

The confocal microscopy results provided the first hint that both surface charge and pegylation can alter each of the kinetic steps that determine the intracellular bioavailability of cationic liposomes. Changes in these properties altered the liposome localization (membrane-bound *vs*. intracellular), intracellular transport (dispersed throughout the cytosol *vs*. clustered near the inner leaf of plasma membrane), and residence in endosomes/lysosomes (e.g., indicated by the increasingly punctated signals). The results further showed different fates of intracellular liposomes when both charge and pegylation were changed separately or jointly, indicating interplay between these property parameters. For example, the combined use of high surface charge and low pegylation (C40-0 and C40-1) showed different kinetics of internalization of membrane-bound liposomes and subsequent processing compared to other charge/pegylation combinations.

Internalization takes place by endocytosis or pinocytosis of the membrane-bound liposome (6). Analysis of I *versus* B values over time indicated steady state was reached at approximately 4 h, at which time I was linearly correlated with B, with a constant I/B ratio for an individual formulation at all medium concentrations (and different I/B ratios for different formulations). As the steady state reflects the net between rate of internalization and rate of efflux/degradation, the concentration-independent I/B ratio suggests first-order rate processes of internalization and efflux.

The process of internalization showed an interesting time dependency, with the I/B ratio peaking at about 1 h for most preparations, followed by a decrease before equilibrium was reached. Because the I/B ratios were normalized for the membrane-bound liposomes, this kinetic behavior suggests an initially faster rate of endocytosis followed by a slower rate (e.g., depletion of receptors over time) or an increase in efflux or degradation of the endocytosed liposomes.

The proportionality constant K represents the I/B ratio at equilibrium, observed essentially unchanged over a large range of medium concentrations. K values showed a positive triphasic relationship with ZP and a negative biphasic relationship with pegylation. These data indicate changes in intracellular bioavailability of liposomes did not always follow changes in their membrane binding. The magnitudes of changes in K values *vs*. surface charge (3-fold) relative to pegylation (~25%) indicate surface charge has a greater weight on determining the membrane binding and intracellular bioavailability such that increasing the charge partially offset the negative consequences of pegylation. The best-fitting linear regression equations (Fig. 6) show the quantitative relationships of the observed TC_{eq}, B_{eq}, and I_{eq} values with ZP and % pegylation and may predict TC_{eq}, B_{eq}, I_{eq} for different formulations.

The combined evaluation of binding and internalization by quantitation of fluorescence and inspection by confocal microscopy provided additional confirmation and insight. Confocal microscopy showed patterns of punctated and diffuse intracellular fluorescence. Punctuated appearance typically indicates presence in endosomes/lysosomes, whereas diffuse fluorescence suggests release from endosomes. Diffuse patterns were most apparent for liposomes of high surface charge plus no or low pegylation. Increasingly punctated signals were observed at higher pegylation, possibly due to the increasing liposome stability. Changes in the appearance of the fluorescence signals further show that the intracellular bioavailability, on its own, cannot predict the efficacy of gene therapy. This is because this measurement does not reflect the level of gene therapeutic released from endosomes, available to exert its action.

Finally, our studies were based on the total fluorescence signals and most of the data analysis was based on the B and I values at equilibrium; the results cannot distinguish between internalization and other intracellular processes such as degradation and efflux. Hence, we were not able to delineate the individual intracellular events that were altered by pegylation or surface charge, e.g., whether these liposome properties affect the endosomal escape or the localization of liposomes (e.g., bound to membrane lipid raft, the inside of the membrane, or cytosol). Additional qualitative and quantitative data on the effects of surface charge and pegylation on these dynamic processes (e.g., range of linearity *vs*. saturability, rate constants for intracellular transport and processing) would be useful to optimize the liposome design to yield maximal intracellular bioavailability of gene therapeutics.

CONCLUSION

Most studies on using cationic liposomes as gene vectors have focused on demonstrating the effects of surface charge and pegylation on the transfection efficiency and mechanisms of transmembrane and intracellular transport. The present study used a kinetic-based approach to study the effects of these liposome properties on the intracellular bioavailability of cationic liposomes. The results show that either property can affect the kinetics of liposome binding to cell membrane, internalization of membrane-bound liposomes, and subsequent intracellular transport and processing (including residence in endosomes). The substantial qualitative and quantitative differences of their effects on these individual processes are such that it may be possible to fine-tune these two properties to achieve an optimal balance of intracellular bioavailability with stealth property.

ACKNOWLEDGEMENTS

This work was supported in part by research grants R43CA134047, R01EB015253 and R01CA158300 from the National Cancer Institute, DHHS. Yinghuan Li is supported by the China Scholarship Council Fellowship. Images used in this article were generated at The Campus Microscopy and Imaging Facility, The Ohio State University.

REFERENCES

1. Wang J, Lu Z, Wientjes MG, Au JL. Delivery of siRNA Therapeutics: Barriers and Carriers. AAPS J. 2010;12(4):492–503.
2. Fisher KD, Ulbrich K, Subr V, Ward CM, Mautner V, Blakey D, *et al*. A versatile system for receptor-mediated gene delivery permits increased entry of DNA into target cells, enhanced delivery to the nucleus and elevated rates of transgene expression. Gene Ther. 2000;7(15):1337–43.
3. Li B, Li S, Tan Y, Stolz DB, Watkins SC, Block LH, *et al*. Lyophilization of cationic lipid-protamine-DNA (LPD) complexes. J Pharm Sci. 2000;89(3):355–64.
4. Tseng YC, Mozumdar S, Huang L. Lipid-based systemic delivery of siRNA. Adv Drug Deliv Rev. 2009;61(9):721–31.
5. Wu SY, McMillan NA. Lipidic systems for *in vivo* siRNA delivery. AAPS J. 2009;11(4):639–52.
6. Khalil IA, Kogure K, Akita H, Harashima H. Uptake pathways and subsequent intracellular trafficking in nonviral gene delivery. Pharmacol Rev. 2006;58(1):32–45.
7. Khalil IA, Kogure K, Futaki S, Harashima H. High density of octaarginine stimulates macropinocytosis leading to efficient intracellular trafficking for gene expression. J Biol Chem. 2006;281(6):3544–51.
8. Iyer AK, Khaled G, Fang J, Maeda H. Exploiting the enhanced permeability and retention effect for tumor targeting. Drug Discov Today. 2006;11(17–18):812–8.
9. Gabizon A, Shmeeda H, Barenholz Y. Pharmacokinetics of pegylated liposomal Doxorubicin: review of animal and human studies. Clin Pharmacokinet. 2003;42(5):419–36.
10. Dos Santos N, Allen C, Doppen AM, Anantha M, Cox KAK, Gallagher RC, *et al*. Influence of poly(ethylene glycol) grafting density and polymer length on liposomes: Relating plasma circulation lifetimes to protein binding. Biochim Biophys Acta. 2007;1768(6):1367–77.
11. Kenworthy AK, Hristova K, Needham D, McIntosh TJ. Range and magnitude of the steric pressure between bilayers containing phospholipids with covalently attached poly(ethylene glycol). Biophys J. 1995;68(5):1921–36.
12. Li SD, Huang L. Pharmacokinetics and biodistribution of nanoparticles. Mol Pharm. 2008;5(4):496–504.
13. Ma Z, Li J, He F, Wilson A, Pitt B, Li S. Cationic lipids enhance siRNA-mediated interferon response in mice. Biochem Biophys Res Commun. 2005;330(3):755–9.
14. Zhang Y, Anchordoquy TJ. The role of lipid charge density in the serum stability of cationic lipid/DNA complexes. Biochim Biophys Acta. 2004;1663(1–2):143–57.
15. Porteous DJ, Dorin JR, McLachlan G, Davidson-Smith H, Davidson H, Stevenson BJ, *et al*. Evidence for safety and efficacy of DOTAP cationic liposome mediated CFTR gene transfer to the nasal epithelium of patients with cystic fibrosis. Gene Ther. 1997;4(3):210–8.
16. Simoes S, Moreira JN, Fonseca C, Duzgunes N, de Lima MCP. On the formulation of pH-sensitive long circulation times. Adv Drug Deliv Rev. 2004;56(7):947–65.

17. Yang T, Cui FD, Choi MK, Cho JW, Chung SJ, Shim CK, *et al*. Enhanced solubility and stability of PEGylated liposomal paclitaxel: *in vitro* and *in vivo* evaluation. Int J Pharm. 2007;338 (1–2):317–26.
18. Hobbs SK, Monsky WL, Yuan F, Roberts WG, Griffith L, Torchilin VP, *et al*. Regulation of transport pathways in tumor vessels: Role of tumor type and microenvironment. Proc Natl Acad Sci USA. 1998;95(8):4607–12.
19. Yuan F, Dellian M, Fukumura D, Leunig M, Berk DA, Torchilin VP, *et al*. Vascular-Permeability in A Human Tumor Xenograft - Molecular-Size Dependence and Cutoff Size. Cancer Res. 1995;55(17):3752–6.
20. Duzgunes N, Nir S. Mechanisms and kinetics of liposome-cell interactions. Adv Drug Deliv Rev. 1999;40(1–2):3–18.
21. Lee KD, Nir S, Papahadjopoulos D. Quantitative analysis of liposome-cell interactions *in vitro*: rate constants of binding and endocytosis with suspension and adherent J774 cells and human monocytes. Biochemistry. 1993;32(3):889–99.
22. Wrobel I, Collins D. Fusion of cationic liposomes with mammalian cells occurs after endocytosis. Biochim Biophys Acta. 1995;1235(2):296–304.
23. Qaddoumi MG, Ueda H, Yang J, Davda J, Labhasetwar V, Lee VHL. The characteristics and mechanisms of uptake of PLGA nanoparticles in rabbit conjunctival epithelial cell layers. Pharm Res. 2004;21(4):641–8.
24. Hinrichs WL, Mancenido FA, Sanders NN, Braeckmans K, De Smedt SC, Demeester J, *et al*. The choice of a suitable oligosaccharide to prevent aggregation of PEGylated nanoparticles during freeze thawing and freeze drying. Int J Pharm. 2006;311(1–2):237–44.
25. Gjetting T, Arildsen NS, Christensen CL, Poulsen TT, Roth JA, Handlos VN, *et al*. *In vitro* and *in vivo* effects of polyethylene glycol (PEG)-modified lipid in DOTAP/cholesterol-mediated gene transfection. Int J Nanomedicine. 2010;5:371–83.
26. Rejman J, Bragonzi A, Conese M. Role of clathrin- and caveolae-mediated endocytosis in gene transfer mediated by lipo- and polyplexes. Mol Ther. 2005;12(3):468–74.
27. Miller CR, Bondurant B, Mclean SD, McGovern KA, O'Brien DF. Liposome-cell interactions *in vitro*: Effect of liposome surface charge on the binding and endocytosis of conventional and sterically stabilized liposomes. Biochemistry. 1998;37 (37):12875–83.
28. Santel A, Aleku M, Keil O, Endruschat J, Esche V, Fisch G, *et al*. A novel siRNA-lipoplex technology for RNA interference in the mouse vascular endothelium. Gene Ther. 2006;13(16):1222–34.